ELSEVIER

Ceramics International 28 (2002) 327–335

CERAMICS INTERNATIONAL

www.elsevier.com/locate/ceramint

Synthesis of strontium cerates-based perovskite ceramics via water-soluble complex precursor routes

Shaomin Liu[a], Xiaoyao Tan[b], K. Li[b,*], R. Hughes[c]

[a]*Department of Chemical and Environmental Engineering, National University of Singapore, 10 Kent Ridge Crescent Singapore 119260, Singapore*
[b]*Department of Chemical Engineering, University of Bath, Claverton Down, Bath BA2 7AY, UK*
[c]*Department of Chemical Engineering, University of Salford, Salford M4, UK*

Received 28 July 2001; received in revised form 27 August 2001; accepted 4 September 2001

Abstract

Strontium cerates-based ceramic powders, $SrCe_{1-x}M_xO_{3-\alpha}$ ($x=0.05$, $M=$Yb, Y, In, Ga, La) containing a single perovskite phase have been synthesized via water-soluble complex precursor routes using ethylenediaminetetraacetic acid (EDTA), citric acid or glycine as a chelating ligand. The effects of the chelating agent on the synthesis and the evolution of crystalline phase as well as the characteristics of ceramic powders have been investigated in detail. Experimental results indicate that a sintering temperature of 950–1000 °C, which is much lower than that for the conventional solid state reaction process, is sufficient to the formation of clean single perovskite phase. The amount of chelating ligand needed for preparing ceramic powders decreases in the order: citric acid method > glycine method > EDTA method. The particle size of ceramic powders increases with increasing the sintering temperature. Citric acid is a more effective chelating ligand than EDTA and glycine in producing fine ceramic powder with a temperature lower than 1000 °C.

Keywords: Ceramic powders; Perovskite oxides; Complexes

1. Introduction

Proton-conducting ceramics are promising materials for future energy saving and environmental conservation, since they can be applied to many devices for energy conversion, production and separation of hydrogen, synthesis of chemicals, sensing of hydrogen-containing compounds etc. Since 1981 when Iwahara et al. [1] demonstrated that some doped-$SrCeO_3$ ceramics show proton conduction, an increased interest in developing new high temperature proton-conducting ceramics and studying their proton-conducting properties has been generated [1–3]. Up to now, a series of perovskite oxides have been reported to exhibit appreciably high proton conduction and their conduction properties have been studied by many investigators [4–10]. Most of these perovskite oxides can be described by the general stoichiometric formula of $AB_{1-x}M_xO_{3-\alpha}$ where A is Ca, Sr or Ba; B is selected from a group consisting of Ce, Zr, Tb or Th; M is some trivalent dopant such as Yb, Y, Dy, In, La, Nd, Ga and Gd; and α is the number of oxygen deficiencies per unit formula of the perovskite-type oxide, although other complex perovskites in the forms of $A_2B'B''O_6$ and $A_3B'B''_2O_9$ also exhibit proton-conducting properties [11]. Among them, strontium cerium trioxide ($SrCeO_3$)-based oxide composites, for example, $SrCe_{0.95}Yb_{0.05}O_{3-\alpha}$, shows highest proton conductivity and chemical stability and, therefore, have spurred more interest [2].

In general, applications of the ionic conducting materials always start with the synthesis of the corresponding ceramic powders, and the conventional solid state reaction route is often applied. In this method, the starting materials, $SrCO_3$ and other metal oxides, mixed in a stoichiometric ratio to yield the given composition, are ball-milled, ground and fired at a high temperature. Such a synthesis method often leads to the following disadvantages: (1) a micro-homogenous phase structure can hardly be obtained due to large and strongly bonded powder agglomerates; (2) contamination can hardly be avoided during milling and grinding, resulting in a detrimental effect on the material properties; and (3) the mechanically ground mixture requires prolonged

* Corresponding author. Tel.: +44-1225-826372; fax: +44-1225-826894.
E-mail address: k.li@bath.ac.uk (K. Li).

0272-8842/02/$22.00
PII: S0272-8842(01)00098-0

calcination at high temperatures (usually > 1400 °C), which is undesirable in the fabrication of dense fine-grained ceramics due to the promotion of abnormal crystallite growth. Consequently, both the electrical and mechanical properties of the final sintered ceramic products by the conventional standard method are not adequate for many advanced applications. In order to obtain homogeneous fine powders, other different methods via various solution-routes such as freeze-drying [12], co-precipitation [13] and combustion of metal-organic precursors [14,15], have been proposed. Among these techniques, the combustion method based on water-soluble chelated complexes as precursors to obtain the homogeneity of the metal ion distribution on the atomic level [14], is currently attracting considerable attention. Such a water-soluble complex precursor synthesis route has shown to be advantageous for obtaining carbonate-free, chemical homogeneous oxide compounds with a high relative density and a high bending strength [15].

Chelating ligands which contain carboxylate groups or carboxylate and aliphatic amine groups are essential in the water-soluble complex precursor synthesis route. Citric acid (containing carboxylate groups), glycine and ethylenediaminetetraacetic acid (EDTA) (containing carboxylate and aliphatic amine groups) were often used before in the synthesis of oxide conducting ceramic powders. In this study, such a technique has been used to synthesize proton-conducting strontium cerates-based ceramics powders, $SrCe_{1-x}M_xO_{3-\alpha}$ ($x = 0.05$, M = Yb, Y, In, Ga, La) with a pure perovskite structure, where different chelating ligand such as citric acid, glycine and EDTA has been tested. The effects of chelating agents on the synthesis procedure and the evolution of crystalline phase as well as the characteristics of ceramic powders have been investigated in detail.

2. Experimental

2.1. Chemicals

$Ce(NH_4)_2(NO_3)_6$ (> 98.7%, Sigma), $SrCO_3$ (> 99.9%, Strem), glycine (> 99.7%, Merk), citric acid (> 99%, Ajax), Ethylenediaminetetraacetic acid (EDTA, > 99.5%, Aldrich), $Yb(NO)_3{\cdot}5H_2O$ (> 99.9%, Strem), $In(NO)_3{\cdot}5H_2O$ (> 99.9%, Aldrich), $Ga(NO)_3{\cdot}6H_2O$ (> 99.9%, Aldrich), $La(NO)_3{\cdot}6H_2O$ (> 99.99%, Aldrich), $Y(NO)_3{\cdot}6H_2O$ (> 99.9%, Aldrich)

2.2. Synthesis of ceramic powders

$SrCeO_3$-based ceramic powders were synthesized by the complex precursor method as summarized in Fig. 1. The synthesis procedures using different chelating ligands, named EDTA method, citric acid method and glycine method, respectively, are described as follows.

2.2.1. EDTA method

EDTA powder was introduced with magnetic stirring into distilled water placed in a 400 ml beaker. Aqueous ammonia was then added to the beaker to facilitate the dissolution of EDTA, forming a water-soluble ammonium salt. The resulting solution had a pH of 8–10 and was labelled as solution A. In a separate beaker, stoichiometric amounts of $SrCO_3$ powder, $Ce(NH_4)_2(NO_3)_6$ and corresponding dopant, (metal nitrates like $Yb(NO)_3{\cdot}5H_2O$, $Y(NO)_3{\cdot}6H_2O$, $In(NO)_3{\cdot}5H_2O$, $Ga(NO)_3{\cdot}6H_2O$ or $La(NO)_3{\cdot}6H_2O$) were dissolved in distilled water, resulting in another solution (yellow-colored) labeled as solution B. The solution B was then added drop by drop to the solution A to avoid irreversible precipitation. After the addition of the solution B to the solution A was completed, the whole mixture was stirred at 80 °C for several hours until the solution became completely transparent, containing metal ion and EDTA complexes. The transparent solution was further heated at 90 °C overnight to remove excess water and promote polymerization. During continued heating, the solution became more viscous with a change of colour from colourless to yellow but without any visible formation of precipitation or turbidity. The resulting dried gel was a yellow transparent resin. A portion of the resin was pyrolized at 200–350 °C for 2 h in a carbolite furnace, resulting in a black solid mass, which was lightly ground into powder, called precursor. This operation was carried out strictly in a well-ventilated fume hood to prevent gases and ashes from being inhaled. Under an airflow (2 l/min), the powder precursor was heat-treated or calcined at 600–1300 °C to remove residual carbon and form the desired structure.

2.2.2. Citric acid and glycine methods

Citric acid or glycine instead of EDTA was added in granular form as the complexing agent, together with appropriate proportions of $SrCO_3$ powder, $Ce(NH_4)_2(NO_3)_6$, $M(NO_3)_3{\cdot}xH_2O$. The optimum temperature for pyrolysis of intermediate resin to get powder precursor by this method should be at 300–350 °C and 190–210 °C, respectively. The exposure of powder precursors to atmosphere would lead to absorption of water, particularly for those prepared by glycine methods. Therefore the powder precursors should be preserved under moisture-proof condition.

2.3. Characterisation techniques

2.3.1. Thermal analysis

Thermogravimetric analysis (TGA) was carried out by a TA instrument (TGA 2050). Fifteen milligrams of sintering powder was placed in sample holder and heated from 25 to 1000 °C at a rate of 5 °C/min in air (flow rate = 90 ml/min), while weight change was recorded as function of temperature. Differential thermal analyses

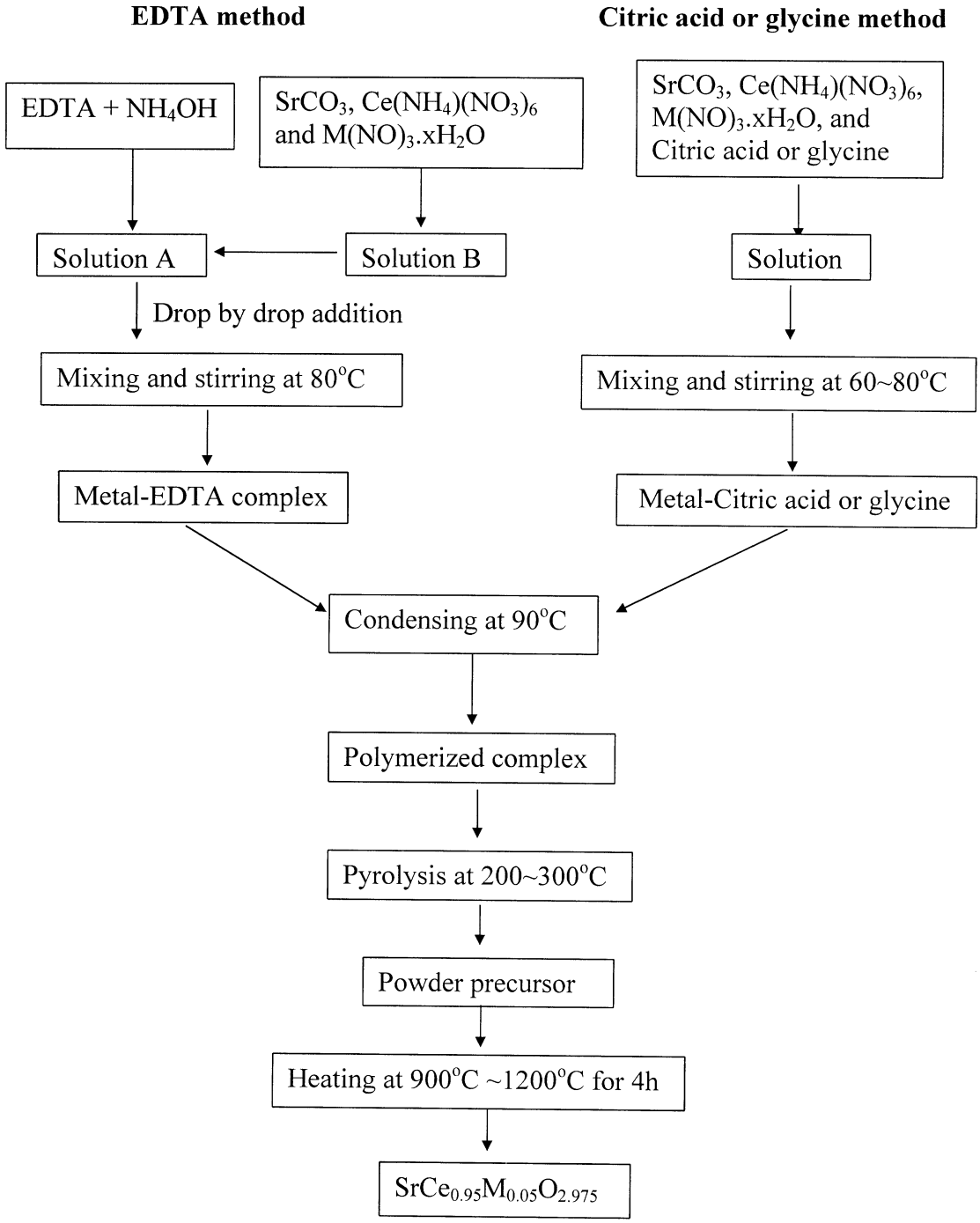

Fig. 1. Flow chart illustrating the processing procedure for the preparation of $SrCe_{0.95}M_{0.05}O_{2.975}$ (M = Yb, Y, In, La, Ga) powders.

(DTA) were performed in a Perkin-Elmer DTA instrument. Five milligrams of sample was used and heated from 25 to 1000 °C at a rate of 5 °C/min in air or nitrogen (flow rate = 30 ml/min), while heat flux changes were also recorded as a function of temperature.

2.3.2. XRD measurement

Structural phases were determined for sintering powders in a Shimadzu X-ray diffractometer using Cu$K\alpha$ radiation. A continuous scan mode was used to collect 2θ data from 10 to 80° with a 0.02 sampling pitch and a 2°/min scan rate. X-ray tube voltage and current were set at 40 kV and 30 mA, respectively.

2.3.3. SEM measurement

Structures of the prepared ceramic powder were visually observed using a scanning electron microscope (Hitachi Model S-4100).

2.3.4. Particle size measurement

The particle size of final sintered powder agglomerates was analysed by 90PLUS particle size analyser. Before the measurement, the powder was ultrasonic-dispersed in water for 2–3 min.

3. Results and discussion

3.1. Determination of the optimum amount of chelating ligand

It is the first step to have a homogeneous intermediate resin for the successful application of the complex precursor technique to produce ceramic powders with desired structures. The powders of the composite obtained from the heterogeneous resins (for example, precipitation occurs in condensing the chelating precursor solution) would possess an undesired structure after the heat treatment.

The amount of chelating ligand plays an important role in keeping the resin homogeneous. The content of chelating ligand should be high enough to prevent precipitation occurring over the entire concentration process, otherwise the compositional homogeneity of the three metal ions in the aqueous solutions could not be well maintained, on a molecular scale, in the resulting gels. On the other hand, since all organic components involved will be eventually burned off, it is desirable to minimize their concentration and hence the cost. Therefore, one process variable investigated in this study is the minimum molar ratio of chelating ligand to total metal ions (defined as R). Depending on the metal ions and chelating ligands, the suggested values of R and characteristics of the obtained gels are given in Table 1. For solutions with the ratio lower than R, it was difficult to keep the metal ions in solution and irreversible precipitation usually occurred during the evaporation of the mixed solution due to the lack of a sufficient amount of chelating ligand molecules. Once the precipitation occurred, adjustment of the pH of the solutions by addition of an acid or a base would not help in dissolution of metal salts. From Table 1, it can be seen that the R value of EDTA and glycine methods is usually lower than that of the citric acid method. This is because that EDTA and glycine containing both of carboxylate and aliphatic amine groups to participate in the complexation of metal ions have stronger chelating ability than citric acid, which contains only carboxylate groups. Similar data were also obtained by Agarwal et al. [16], who studied barium cerate-based composites in their work. The low chelating ability of citric acid is also verified by the requirement of strict concentration conditions. If the water evaporation rate is very high, white-yellow irreversible precipitation takes place and the solution would become a paste. Therefore, when using the citric acid process to obtain a transparent intermediate resin of oxide, the condensing temperature should not be above 70 °C until the formation of a highly viscous gel. Contrary to citric acid process, the condensing or evaporation temperature for EDTA and glycine process can be varied at individual request.

3.2. Effect of chelating ligands on the pyrolysis of complex precursors

The histories of the pyrolysis processes of the complex precursors were recorded by TGA and DTA as shown in Figs. 2 and 3, respectively. Different combustion reactions were observed during the pyrolysis of these chelating precursors due to the different compositions used. As can be seen in Fig. 2, the TGA curves show a three-stage weight loss profile. The first stage of the TGA profile having a span of 30–100 °C is attributed to

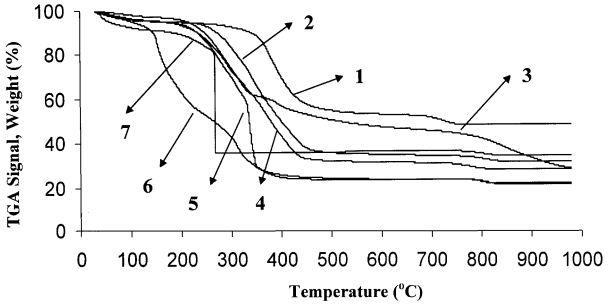

Fig. 2. TGA curves: 1, $SrCe_{0.95}Ga_{0.05}O_{2.975}$, EDTA (in air); 2, $SrCe_{0.95}In_{0.05}O_{2.975}$, citric acid (in air); 3, $SrCe_{0.95}Yb_{0.05}O_{2.975}$, EDTA (in nitrogen); 4, $SrCe_{0.95}Y_{0.05}O_{2.975}$, citric acid (in air); 5, $SrCe_{0.95}Yb_{0.05}O_{2.975}$, EDTA (in air); 6, $SrCe_{0.95}Yb_{0.05}O_{2.975}$, citric acid (in air); 7, $SrCe_{0.95}Yb_{0.05}O_{2.975}$, glycine (in air).

Table 1
The minimum R for preparation of $SrCe_{1-x}M_xO_{3-\alpha}$ ($x=0.05$) chelating precursors and characterisation of resulting dried intermediate resins

Methods	R ratio[a]				
	$SrCe_{0.95}Yb_{0.05}O_{3-\alpha}$	$SrCe_{0.95}Y_{0.05}O_{3-\alpha}$	$SrCe_{0.95}In_{0.05}O_{3-\alpha}$	$SrCe_{0.95}Ga_{0.05}O_{3-\alpha}$	$SrCe_{0.95}La_{0.05}O_{2.975}$
EDTA	1.2 (O, yellow)	2.5 (O, yellow)	2.5 (O, yellow)	1.5 (O, yellow)	1.5 (O, yellow)
Glycine	1.2 (O, black-red)	3.0 (O, black-red)	2.5 (O, black-red)	2.0 (O, green-white)	2.5 (O, black-red)
Citric acid	4.0 (T, yellow)	4.0 (T, yellow)	4.0 (T, yellow)	4.0 (T, yellow)	4.0 (T, yellow)

[a] T, transparent; O, opaque.

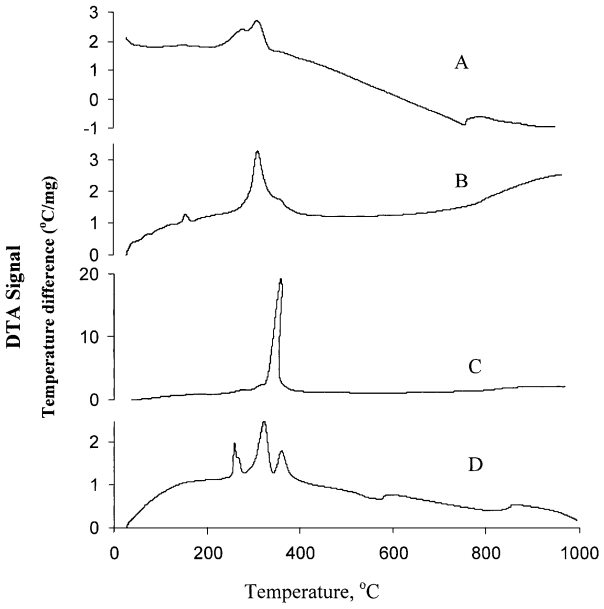

Fig. 3. DTA curves of the $SrCe_{0.95}Yb_{0.05}O_{2.975}$ precursors prepared by three methods: (A) EDTA method in nitrogen; (B) EDTA method in air; (C) citric acid in air; and (D) glycine method in air.

the loss of water, since the intermediate resins are not dried completely and easily absorb water. The second stage, a fast weight loss stage claimed about 65% in the range of 200–500 °C, is due to the decomposition of the related coordination species, corresponding to the high exothermic peaks at 300 or 350 °C in DTA curves (B and C in Fig. 3). The third stage is a gradual weight loss stage, with more obvious weight loss between 750 and 800 °C and subsequent XRD analysis has shown that this is due to the thermal decomposition of carbonates.

Pyrolysis of the chelating precursor made from glycine was an explosive process because the large amount of gases was released instantaneously with a loud sound when the temperature of furnace, where 20 g of the precursor was placed, was increased to 250 °C. Therefore, combustion of large quantities of such a precursor should be undertaken with extreme caution. From the TGA of the glycine precursors (curve 7 in Fig. 2), it can be seen that an unusual weight-loss profile takes place at the temperature of 240 °C. As an evidence of explosive and gaseous pyrolytic process, SEM of the powder agglomerates prepared from glycine has a porous snowflake-like particulate structure as shown in Fig. 4. Subsequent XRD analysis indicates that $Sr(NO_3)_2$ exists in the powder precursors prepared at the temperature of 200 °C as shown in Fig. 5(a). However, there is no $Sr(NO_3)_2$ detected in the powder precursors prepared by EDTA and citric acid methods (Fig. 6). It has been verified that the presence of free $Sr(NO_3)_2$, which is a very strong oxidizing agent while heated together with reducing agents [17], is the reason to have the explosive combustion. The explosive mechanism behind the combustion may involve the formation of highly oxidative

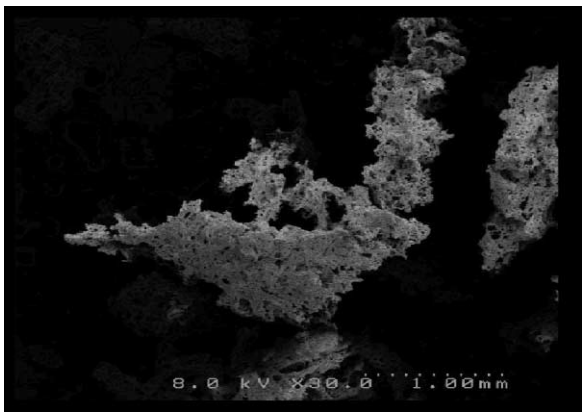

Fig. 4. Scanning electron micrographs of $SrCe_{0.95}Yb_{0.05}O_{2.975}$ sintering at 1300 °C (glycine method).

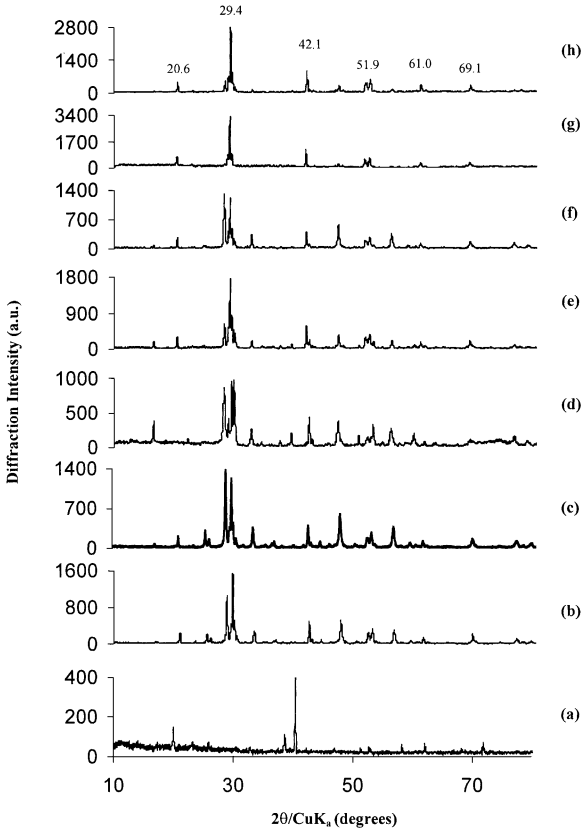

Fig. 5. XRD analysis for $SrCe_{0.95}Yb_{0.05}O_{2.975}$ prepared by glycine method at different sintering temperatures: (a) powder precursor, (b) 400 °C 4 h, (C) 700 °C 4 h, (d) 800 °C 17 h, (e) 900 °C 4 h, (f) 950 °C 4 h, (g) 1000 °C 4 h, (h) 1100 °C 4 h.

species,NO_2^+ with the assistance of Sr(II) ion. NO_2^+ reacts rapidly with organic compounds to form organic nitrates [18] and these organic nitrates are often very heat-unstable compounds, i.e. nitroglycerine and trinitrotoluene. The same explosive phenomenon was also observed by Guo [19] in preparing $La_{0.05}Sr_{0.95}CoO_{2.025}$ powders by the glycine method.

Comparing TGA curves of powder precursors prepared by the three methods, it is interesting to note that

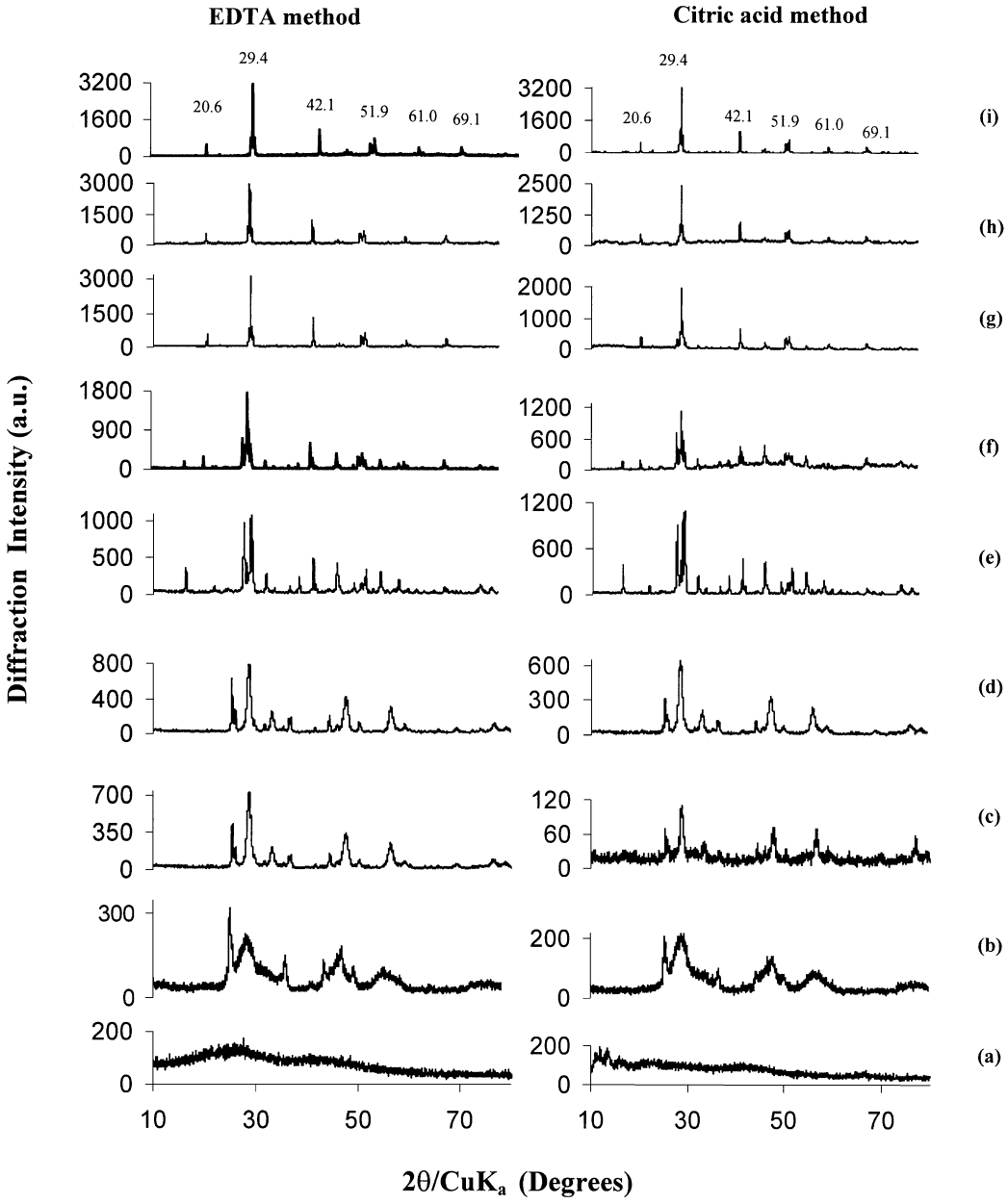

Fig. 6. XRD analysis for $SrCe_{0.95}Yb_{0.05}O_{2.975}$ powder sintered at different temperatures: (a) powder precursor, (b) 400 °C 4 h, (C) 600 °C 4 h, (d) 700 °C 4 h, (e) 800 °C 24 h, (f) 900 °C 4 h, (g) 950 °C 4 h, (h) 1000 °C 4 h, (i) 1100 °C 4 h.

their final weight loss stages are all focused at about 800 °C at which a relative larger amount of carbonate decomposition to oxide occurred, followed by crystallization at a higher temperature. This corresponds to the endothermic peaks followed by exothermic peaks round the temperature of 800 °C, as shown in Fig. 3(D). The endothermic and exothermic peaks around 800 °C in DTA curves of Fig. 3(B) and (C) do not appear. This may be due to the amount of carbonates being decomposed at this temperature to be not large enough. However, the DTA curves (in nitrogen) of the powder precursor did possess similar endothermic and exothermic peaks around 800 °C as shown in Fig. 3(A). The weight loss stage due to carbonates decomposition over the same temperature range was also observed by other investigators [20,21] for fabricating oxide composites containing strontium oxide.

3.3. Effects of chelating ligands on structural evolution of $SrCe_{1-x}M_xO_{3-\alpha}$ compounds

Crystalline $SrCe_{1-x}M_xO_{3-\alpha}$ ($x=0.05$, $M=$Yb, Y, In, La, Ga) oxides were obtained by calcination of the obtained powder precursors at higher temperatures. The development of the crystalline phase as a function of calcining temperature is illustrated by the XRD patterns

plotted in Figs. 5 and 6, which are based on $SrCe_{0.95}Yb_{0.05}O_{3-\alpha}$ powder precursor. In order to identify the intermediate phases easily, the XRD patterns of some commercially available compounds, such as, $SrCO_3$, CeO_2 and $Sr(NO_3)_2$, etc. were also taken. The characterisation of SrO crystalline phase was based on previous literature [22].

It is interesting to note that the development of crystalline phases of powder precursors fabricated by the three methods is almost in the same trend, particularly at temperatures higher than 800 °C. The starting powder precursors obtained at low temperatures (200–350 °C) were primarily amorphous in structure, as is characterized by the broad continuum (Fig. 6a) and no intermediate products were detectable in the ashes prepared by EDTA and citric acid methods. However, intermediate products, such as uncoordinated strontium nitrate, $Sr(NO_3)_2$ and other unknown phases, were found in the ash prepared by glycine method, as shown in Fig. 5(a).

Powders calcined at 400, 600 and 700 °C were composed of carbonates ($SrCO_3$) and oxides (CeO_2), as shown in Fig. 6(b–d). However, the XRD spectra of powders prepared by the glycine method indicate that cubic perovskite $SrCe_{0.95}Yb_{0.05}O_{3-\alpha}$, CeO_2 and $SrCO_3$ phases coexist, as shown in Fig. 5(b) and (c). At sintering temperatures of 800 °C and 900 °C, the XRD patterns of powders prepared by these three methods display the existence of $SrCe_{0.95}Yb_{0.05}O_{3-\alpha}$, CeO_2 and SrO crystal phases and the disappearance of $SrCO_3$ phases (shown in Fig. 6e, f, and Fig. 5d, e). At sintering temperature above 950 °C, the XRD spectra exhibit the same pattern having seven strong diffraction peaks with respective 2θ angles of 20.6, 29.4, 42.1, 51.9, 52.6, 61, and 69.1, which have previously been related to the cubic perovskite phase of $SrCe_{0.95}Yb_{0.05}O_{3-\alpha}$ [23,24], as shown in Fig. 5(f–h) and in Fig. 6(g–i). The crystalline phases detected by the X-ray diffraction technique in the sintered products are summarized in Table 2.

Based on the XRD, TGA and DTA results, it is clear that the formation of the perovskite structure of $SrCe_{0.95}Yb_{0.05}O_{3-\alpha}$ involves many intermediate phases, which are very temperature dependent. At a sintering

Table 2
Phases (identified by X-ray diffraction analysis) changes of $SrCe_{0.95}Yb_{0.05}O_{3-\alpha}$ powder precursors sintered at different temperatures

Methods	Temperature (°)[a]								
	200–300	400	600	700	800	900	950	1000	1100
EDTA	Amorphous	$SrCO_3$, CeO_2	$SrCO_3$, CeO_2	$SrCO_3$, CeO_2	SrO, CeO_2, SCY	SrO, CeO_2, SCY	SCY	SCY	SCY
Citric acid	Amorphous	$SrCO_3$, CeO_2	$SrCO_3$, CeO_2	$SrCO_3$, CeO_2	SrO, CeO_2, SCY	SrO, CeO_2, SCY	SCY	SCY	SCY
Glycine	$Sr(NO_3)_2$, CeO_2, etc.	$SrCO_3$, CeO_2, SCY	$SrCO_3$, CeO_2, SCY	$SrCO_3$, CeO_2, SCY	SrO, CeO_2, SCY	SrO, CeO_2, SCY	SCY	SCY	SCY

[a] SCY, $SrCe_{0.95}Yb_{0.05}O_{3-\alpha}$.

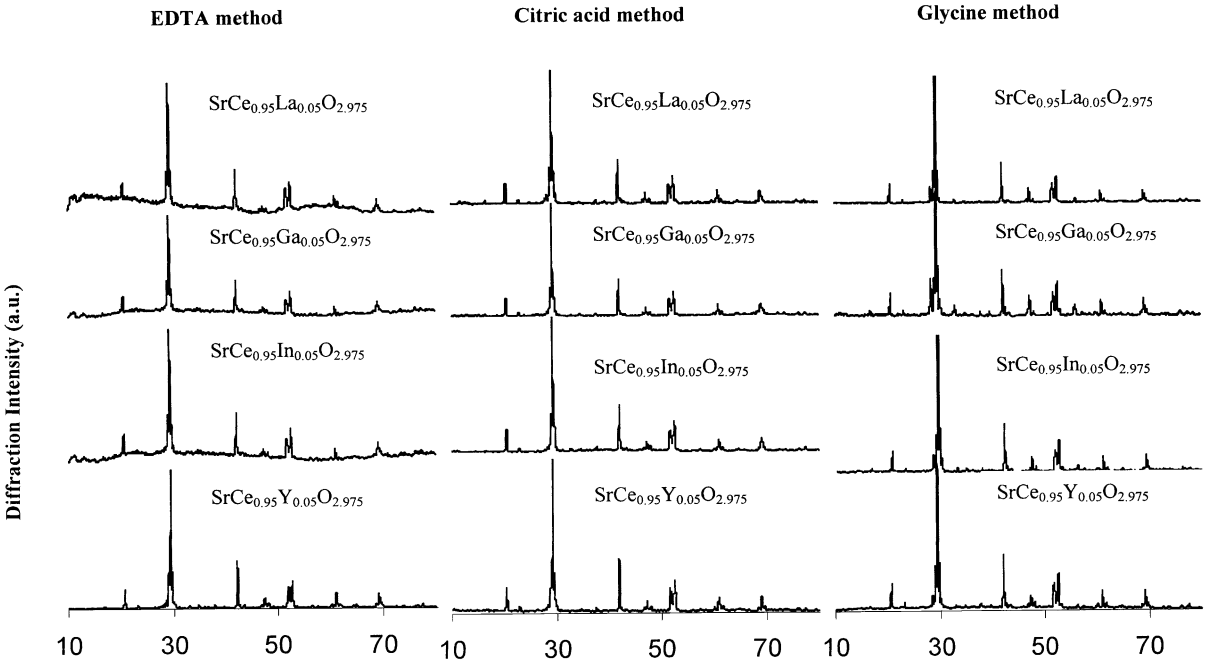

Fig. 7. XRD patterns of $SrCe_{0.95}M_{0.05}O_{2.975}$ (M = Y, In, Ga, and La) fabricated by EDTA, citric acid, and glycine methods (sintered at 1000 °C).

temperature higher than 950 °C, the crystal development of sintered powders is symbolized by the desired single-phase perovskite structure. It, thus, suggests that a sintering temperature higher than 950 °C is required to obtain $SrCe_{0.95}M_{0.05}O_{3-\alpha}$ with pure cubic perovskite structure. Fig. 7 depicts the XRD patterns of $SrCe_{0.95}Y_{0.05}O_{3-\alpha}$, $SrCe_{0.95}In_{0.05}O_{3-\alpha}$, $SrCe_{0.95}Ga_{0.05}O_{3-\alpha}$, and $SrCe_{0.95}In_{0.05}O_{3-\alpha}$ synthesised at a temperature of 1000 °C. It can be seen that all the sintered powders exhibit peaks corresponding to the desired single-phase cubic perovskite structures. Such a structure is not possible to be achieved by the conventional solid state reaction method unless the temperature is increased to 1400 °C with prolonged sintering time.

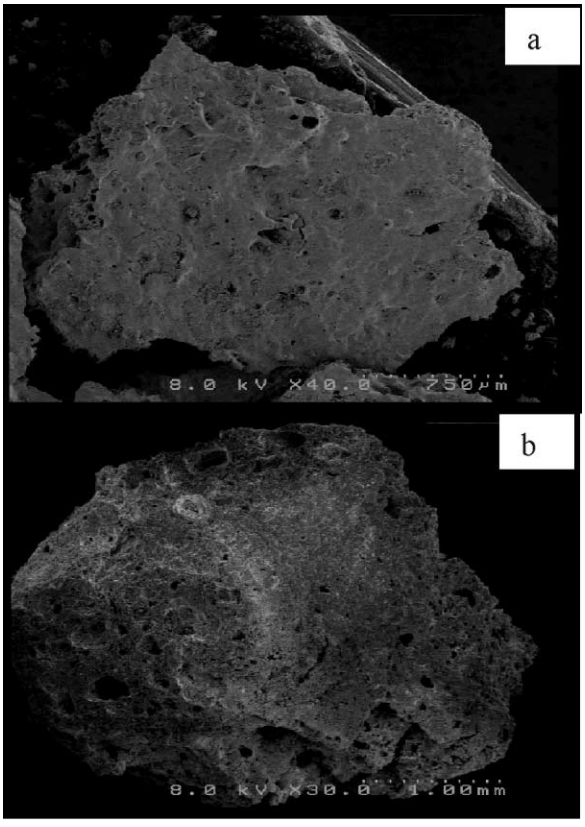

Fig. 8. Scanning electron micrographs of $SrCe_{0.95}Yb_{0.05}O_{2.975}$ sintering at 1300 °C. (a) EDTA method, (b) citric acid method.

3.4. Effect of chelating ligands on the powder characteristics

Representative scanning electron micrographs of $SrCe_{0.95}M_{0.05}O_{3-\alpha}$ ceramic powders fabricated using three different chelating ligands are shown in Figs. 4 and 8. Due to the rapid explosive pyrolysis and the high flame temperature, the powder agglomerates prepared by the glycine method have a more porous structure, as shown in Fig. 4. By comparison, using EDTA and citric acid as chelating ligand would produce larger, harder and denser powder agglomerates connected each other as shown in Fig. 8, since their pyrolysis processes are very sluggish and gases are released out slowly. The average particle size data given in Tables 3 and 4 obtained by the particle size analyser shows that the grain size of powders increases with the increase of sintering temperature. For example, at 1000 °C, the average particle size usually ranges between 0.4 and 0.6 μm (Table 3). However, when the sintering temperature is increased to 1300 °C, abnormal crystal growth was observed and the average particle size is increased to 1.0–1.1 μm (Table 4). Further, the particle size from the citric acid method is generally smaller than from the other two methods, especially when the sintering temperature is lower than 1100 °C. Use of citric acid as the chelating ligand is more effective to produce fine strontium cerates-based ceramic powders.

Table 3
Average particle size (nm) of $SrCe_{1-x}M_xO_{3-\alpha}$ ($x=0.05$, $M=$ Y, In, Ga and La) powders after intermediate sintering at 1000 °C

	Compounds			
Process	$SrCe_{0.95}Y_{0.05}O_{3-\alpha}$	$SrCe_{0.95}In_{0.05}O_{3-\alpha}$	$SrCe_{0.95}Ga_{0.05}O_{3-\alpha}$	$SrCe_{0.95}La_{0.05}O_{3-\alpha}$
EDTA particle size (S.E.)	586.6 (41.9)	656.0 (23.4)	568.4 (5.1)	567.3 (24.6)
Glycine particle size (S.E.)	430.3 (15.0)	464.7 (13.7)	1015.9 (46)	497.8 (4.5)
Citric acid particle size (S.E.)	377.2 (5.7)	414.8 (19.9)	438.4 (7.7)	425.4 (10.6)

Table 4
Average particle size (nm) of $SrCe_{0.95}Yb_{0.05}O_{3-\alpha}$ powders after intermediate sintering

	Sintering temperature (°C)				
Methods	950	1000	1100	1200	1300
EDTA particle size (S.E.)	493.6 (5.8)	557.4 (9.8)	751.8 (8.7)	908.9 (5.3)	1079.9 (209.7)
Glycine particle size (S.E.)	406.7 (23.7)	576.4 (13.3)	642.7 (36.8)	805.4 (23.1)	1041.4 (54.9)
Citric acid particle size (S.E.)	396.5 (6.0)	416.6 (9.3)	625.0 (69.5)	862.1(29.6)	1129.0 (94.9)

4. Conclusions

Strontium cerates-based ceramic powders have been synthesized via water-soluble complex precursor routes using EDTA, citric acid and glycine as the chelating ligand, respectively. The following conclusions can be drawn from this study:

1. The amount of chelating ligand needed for preparing strontium cerates-based ceramic powders decreases in the order: citric acid method > glycine method > EDTA method. Furthermore, the condensing temperature in citric acid method should not be above 70 °C until the formation of a highly viscous gel, whereas it can be varied at individual request in EDTA and glycine processes.
2. The use of glycine leads to a fast pyrolysis of ceramic precursor and fast formation of cubic perovskite structure compared to the use of EDTA and citric acid as the chelating ligand. However, a sintering temperature higher than 950 °C is always required whatever chelating ligand is used in order to obtain a pure perovskite structure.
3. Much lower sintering temperature, i.e. 950–1000 °C, than that used in conventional solid state reaction process is possible to produce $SrCe_{1-x}M_xO_{3-\alpha}$ oxide powders with clean single perovskite phase.
4. The particle size of strontium cerates-based ceramic powders increases with the increase of sintering temperature. Furthermore, citric acid is a more effective chelating ligand than EDTA and glycine in producing fine ceramic powders at a sintering temperature lower than 1000 °C.

Acknowledgements

The authors gratefully acknowledge the research funding provided by EPSRC in the United Kingdom (grant No. GR/N38640). A research scholarship provided by National University of Singapore to one of the authors, S.L., is also gratefully acknowledged.

References

[1] H. Iwahara, T. Esaka, H. Uchida, N. Maeda, Proton conduction in sintered oxides and its application to steam eletrolysis for hydrogen production, Solid State Ionics 3/4 (1981) 359.
[2] H. Iwahara, Advanced ceramics for protonics, in F.W. Poulsen, N. Bonanos, S. Linderoth, M. Mogensen, B. Zachau-Christiansen (Eds.), Proceedings of the 17th International Symposium on Materials Science: High Temperature Electrochemistry: Ceramics and Metals, 1996, pp. 13–28.
[3] K.D. Kreuer, On the development of proton conducting materials for technological applications, Solid States Ionics 97 (1997) 1.
[4] H.H. Iwahara, Technological challenges in the application of proton ceramics, Solid State Ionics 77 (1995) 289.
[5] T.T. Sherban, A.S. Nowick, Bulk protonic conduction in Yb-doped $SrCeO_3$, Solid State Ionics 35 (1989) 189.
[6] N. Bonanos, B. Ellis, M.N. Mahmood, Construction and operation of fuel cells based on the solid electrolyte $BaCeO_3$, Solid State Ionics 44 (1991) 305.
[7] R.L.T. Slade, N. Singh, The perovskite type proton conducting solid electrolyte $BaCe_{0.90}Y_{0.10}O_{3-a}$ in high temperature electrochemical cells, Solid State Ionics 61 (1993) 111.
[8] H.W. James, M. Schwartz, A.F. Sammells, US Patent 5821185, 1998.
[9] X. Qi, Y.S. Lin, Electrical conducting properties of proton-conducting terbium-doped strontium cerate membrane, Solid State Ionics 120 (1999) 85.
[10] P.H. Colomban, Latest developments in proton conductors, Ann. Chim. Sci. Mater. 24 (1999) 1.
[11] B. Groß, St. Marion, R. Hempelmann, D. Grambole, F. Herrmann, Proton conducting $Ba_3Ca_{1.18}$ $Nb_{1.82}O_{8.73}$/H2O: Sol–gel preparation and pressure/composition isotherms, Solid State Ionics 1998 109 (1998) 13.
[12] J. Kirchnerova, D.B. Hibbert, Structures and properties of $La_{1-x}Sr_xCoO_3$ prepared by freeze-drying, J. Mater. Sci. 28 (1993) 5800.
[13] P. Cousin, R.A. Ross, Preparation of mixed oxides: a review, Mater. Sci. Eng. A130 (1990) 119.
[14] P. P. Maggio, Us Patent 3330697, 1967.
[15] K.J. de Vries, Electrical and mechanical properties of proton conducting $SrCe_{0.95}Yb_{0.05}O_{3-\alpha}$, Solid State Ionics 100 (1997) 193.
[16] V.V. Agarwal, M. Liu, Preparation of barium cerate-based thin films using a modified Pechini process, J. Mater. Sci. 32 (1997) 619.
[17] S.G. Hibbins, T. Metals, Strontium and strontium compounds, in: J.I. Kroschwitz (Ed.), Encyclopedia of Chemical Technology, Vol. 22, John Wiley, New York, 1997, p. 957.
[18] J. March, Advanced Organic Chemistry, John Wiley, New York, 1992.
[19] F. Guo, From chelating precursors to $La_{0.05}Sr_{0.95}CoO_{3-y}$ oxide, Master thesis, National University of Singapore, 1999.
[20] R.H.E. van Doorn, A. Kruidhof, A. Nijmeijer, L. Winnubst, A.J. Burggraaf, Preparation of perovskite by thermal decomposition of metal-EDTA complexes, J. Mater. Chem. 8 (9) (1998) 2109.
[21] M.S. Baythoun, F.R. Sale, Production of strontium-substituted lanthanum manganite perovskite powder by the amorphous citrate process, J. Mater. Sci. 17 (1982) 2757.
[22] L.G. Liu, W.A. Bassett, Changes of the crystal structure and the lattice parameters of SrO at higher pressure, J. Geophys. Res. 78 (35) (1973) 8470.
[23] J. Guan, S.E. Dorris, U. Balachandran, M. Liu, Transport properties of $BaCe_{0.95}Y_{0.05}O_{3-\alpha}$ mixed conductor for hydrogen separation, Solid State Ionics 100 (1997) 45.
[24] D. Dionysios, X. Qi, Y.S. Lin, G. Meng, D. Peng, Preparation and characterization of proton conducting terbium doped strontium cerate membranes, J. Membr. Sci. 154 (1995) 143.